ISSN 0005-1144
ATKAFF 50(3–4), 152–166(2009)

Marin Despalatović, Martin Jadrić, Božo Terzić

Influence of Saturation on On-line Estimation of Synchronous Generator Parameters

UDK 621.313.32.07
IFAC 5.5.4;3.1.1

Original scientific paper

This paper discusses on-line estimation of rotor body parameters of the synchronous hydro-generator under saturated condition. A new model of the saturated synchronous salient-pole machine, based on the saturated synchronous inductances which are estimated from measured steady-state operating data, is presented. Using this model the excitation disturbance responses of the saturated synchronous generator are simulated. The synthetic data, obtained by these simulations, are used for testing the estimation procedures and models for both the field and damper winding under saturated condition. It is shown that, by comparison with unsaturated condition, estimation models become more complex and estimation procedures are generally less robust. Particularly, when the damper winding is under consideration, it has been shown that the estimation process gives wrong parameters if the machine saturation characteristic obtained by measurements is not perfectly accurate. Results of measurements performed on the 34 MVA generator in the Peruća hydroelectric power plant in Croatia are presented. The paper also discusses the influence of the measurement noise on the estimation process.

Key words: Identification procedures, Parameter estimation, Saturation model, Synchronous machines

Utjecaj zasićenja na identifikaciju parametara sinkronog generatora u pogonu. U radu se razmatra "on-line" estimacija rotorskih parametara sinkronog hidrogeneratora u uvjetima zasićenja. Razvijen je jedan novi model zasićenog sinkronog stroja s istaknutim polovima koji se temelji na mjerenjima sinkronih reaktancija u stacionarnom stanju. Na temelju tog modela simulirani su odzivi zasićenog sinkronog generatora pri promjeni uzbudnog napona. Odzivi dobiveni simulacijom korišteni su za testiranje estimacijskih postupaka i modela u uvjetima zasićenja, kako za uzbudni tako i za prigušni namot. U usporedbi s nezasićenim stanjem, pokazano je da estimacijski modeli postaju kompleksniji dok su estimacijski postupci manje robusni. Napose, kada se razmatra prigušni namot, pokazano je da estimacijski postupak daje pogrešne parametre ako karaketristika zasićenja stroja nije potpuno točna. Prikazani su rezultati mjerenja dobiveni na generatoru snage 34 MVA u hidroelektrani Peruća. U radu se također razmatra utjecaj mjernog šuma na estimacijski postupak.

Ključne riječi: identifikacijski postupci, estimacija parametara, model zasićenja, sinkroni strojevi

1 INTRODUCTION

A valid model of synchronous generators with accurate parameters is essential for a correct analysis of power systems steady-state and dynamic performance. The standard model structures of synchronous generators are specified in IEC and IEEE standards [1,2] and the main problem is to find the parameters of those known structure. The traditional methods of the standard model parameter determination, like short-circuit tests, standstill frequency response and open circuit frequency response, have some shortcomings. The main of them is that these methods do not take into account parameters deviation due to changes of loading level since the tests are mainly carried out when the machine is not in service. Also, the procedures involve costly and time-consuming tests.

To overcome the shortcomings of the traditional methods, and to include nonlinearities due to saturation, on-line identification methods have been suggested [3-20]. In these methods it tries to estimate parameters of the known model structure from on-line measurements during a small or large machine disturbance. Along with the identification strategy, papers differ in the estimation procedure, the model structure and kind of the system disturbance during measurements. The excitation disturbance of the machine is the most convenient since it does not interfere with normal operating conditions.

Validation studies that are commonly conducted to prove the estimated parameters are based on the comparison of simulation and measurement during a large excitation disturbance. Since the damper currents are not mea-

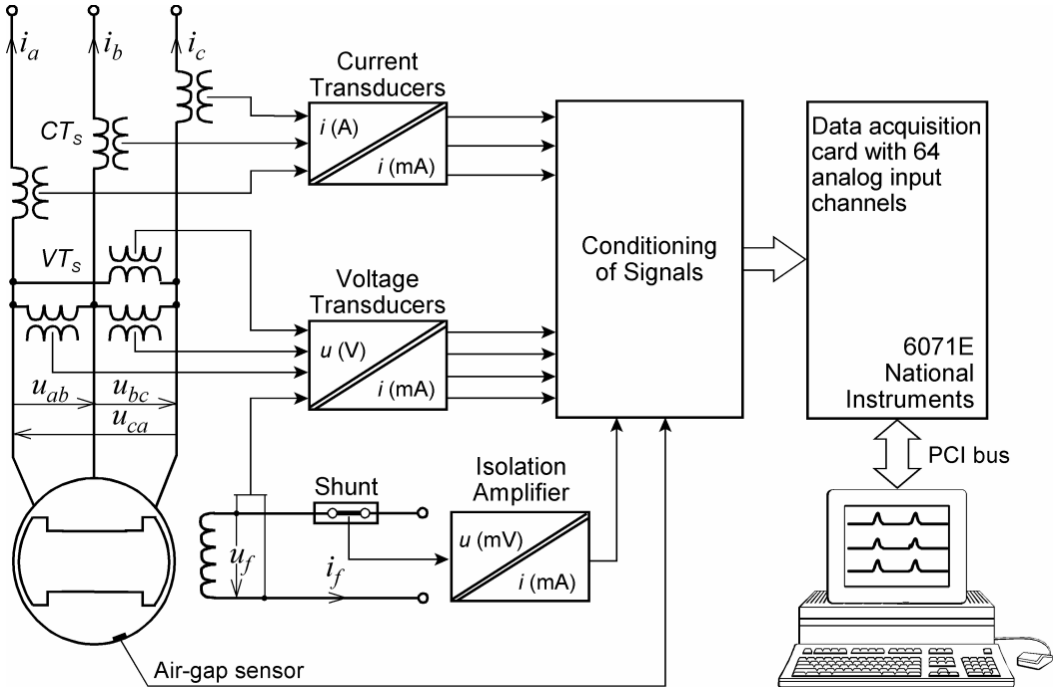

Fig. 1. Measurement configuration installed on 34 MVA generator in HPP Peruća

surable, the question arises if this kind of validation is good enough to prove the damper winding parameters. Namely, during this kind of disturbance, simulated and measured responses of the armature and field currents can match very well with wrong estimates of the damper winding. This could be reason why unacceptable results for the damper winding parameters can be found in some papers. For instance, the damper winding inductance identified in reference [17] is four times bigger than the field winding one. And opposite to that, the damper winding inductance of the synchronous generator is commonly less than the field winding one [21-25].

In this paper the influence of nonlinearity due to saturation on estimation of the rotor body parameters is discussed. A new model of the saturated synchronous machine has been established and used to produce the synthetic data for the investigation purpose. Two different saturation models of the salient-pole synchronous machine have been used to investigate the accuracy and robustness of estimation process under saturated conditions [26,27]. These models are based on the measured saturation characteristics of the 34 MVA generator in the Peruća hydroelectric power plant (HPP). It has been shown that estimation of the damper winding parameters is very sensitive to the accuracy of the saturation characteristics. Practically, a correct estimation of the damper winding parameters is only possible if the identified machine saturation characteristic perfectly matches the actual one.

2 ESTIMATION MODELS OF UNSATURATED MACHINE

In the papers dealing with on-line synchronous machine parameters identification, the procedure is usually divided in two steps [15-19]. The first step of the estimation process involves estimation of the armature circuit parameters and the second step the rotor body parameters. In reference [8] a methodology is presented where estimation of the rotor body parameters is divided in two steps, i.e. the field winding and the damper winding parameters are estimated separately. According to that methodology, separate estimation models for armature, field and damper winding are established. These models are presented below.

The measurement configuration used to provide data for parameter estimation in this study is shown in Fig. 1. In this configuration, the air-gap sensor is used for the power angle measurement which is necessary to obtain the *d*- and *q*-axis terminal voltages (u_d, u_q) and currents (i_d, i_q) [11,18,19,28]. Such a configuration is installed on the 34 MVA generator in HPP Peruća.

2.1 Armature winding

The armature winding estimation model is established in terms of *dq* axis variables assuming that the machine is connected to a power system with balanced conditions, the electrical frequency is constant, and the damper winding currents and the rate of changes of stator flux linkages are

equal zero. The armature resistance can also be neglected when the large machine is under the test. Thus, the following model can be used for estimation of the armature circuit parameters [17-19]

$$\begin{bmatrix} u_d \\ u_q \end{bmatrix} = \begin{bmatrix} 0 & \omega i_q & 0 \\ \frac{2}{3}\omega i_f^* & 0 & -\omega i_d \end{bmatrix} \begin{bmatrix} L_{md}^* \\ L_q \\ L_d \end{bmatrix} \quad (1)$$

where i_f^* is the measured field current, L_{md}^* is product of the field to armature turns ratio (a) and mutual *d*-axis inductance ($L_{md}^* = aL_{md}$), ω is rotor electrical angular velocity, L_d and L_q are synchronous inductances in the *d*- and *q*-axis, respectively. If generator is not under saturated condition, i.e. linearity is satisfied, the parameters L_{md}^*, L_q and L_d are constant and the estimation procedure can be performed to identify them. Thereafter, the value of turns ratio is calculated as follows

$$a = \frac{L_{md}^*}{L_d - L_{\sigma s}} \quad (2)$$

where value of armature leakage inductance ($L_{\sigma s}$) is given by manufacturer-supplied values, or it can be measured by using off-line procedure [1,29].

Thus, the model (1) can be used to identify the armature unsaturated mutual inductance and the turns ratio. If the linearity is not satisfied, the described estimation procedure does not work. To satisfy linearity, in real operating conditions the test data should be generated by conducting a small excitation disturbance with the machine operating at light load and under-excited. This is proposed in references [17-19] as the first stage of the armature parameters estimation.

When $L_{\sigma s}$ and a are known, the saturated synchronous inductances L_d and L_q can be calculated for each steady-state operating point by using the following equations [8]

$$L_d = \frac{U_q + \frac{2}{3}aI_f^*\omega L_{\sigma s}}{\omega\left(\frac{2}{3}aI_f^* - I_d\right)} \quad (3)$$

$$L_q = \frac{U_d}{\omega I_q} \quad (4)$$

where the capital letters denote the steady-state voltages and currents.

For the synchronous machines with high power density it is not possible to achieve linearity at normal operating conditions.Thus, in such cases, the turns ratio can not be estimated by using above described procedure. To overcome this problem the turns ratio can be determined by using an on-line estimation procedure proposed in references [26,27], which is based on the steady-state operating data.

2.2 Field winding

After the armature winding parameters are already determined in the previous step, the field winding resistance (R_f) and leakage inductance ($L_{\sigma f}$) can be estimated by using test data generated by performing a small excitation disturbance caused by a change of the field voltage. In that condition, the damper winding currents and the changes of the stator flux linkages can be neglected and the electrical frequency assumed to be constant. Since the armature winding parameters are known, the following model can be used for estimation of the field winding leakage inductance [8,21-25]

$$\Delta u_f = R_f \Delta\hat{i}_f + \frac{d\Delta\psi_f}{dt} \quad (5)$$

$$\Delta\hat{i}_f = \frac{1}{\hat{L}_{\sigma f} + k_d L_{\sigma s}}\left(\Delta\psi_f - \frac{k_d \Delta u_q}{\omega}\right) \quad (6)$$

where u_f is the field voltage, ψ_f is the field winding flux linkage, and

$$k_d = \frac{L_{md}}{L_{\sigma s} + L_{md}} \quad (7)$$

Note that in above expressions the small-displacements of the machine variables are introduced in order to avoid the calculation of the initial condition for ψ_f. If the linearity is satisfied, all parameters in (5)-(7) are constant and the estimation procedure can be performed in order to identify $L_{\sigma f}$. The field winding resistance is determined by on-line measurements under steady-state conditions. In (5) and (6), Δu_f and Δu_q are the measured input variables; $\Delta\hat{i}_f$ is the estimated output variable and $\Delta\psi_f$ is the state variable with the zero initial value.

2.3 Damper winding

The damper winding parameters are estimated in the last step when the parameters of the armature and the field winding are already identified. The only allowed assumption is that the electrical frequency is constant. Under unsaturated condition and without measurement noise, the damper winding parameters (R_D, $L_{\sigma D}$, R_Q, $L_{\sigma Q}$) can be estimated by using the test data generated by conducting a small excitation disturbance caused by a sudden change of the field voltage. Using measured variables u_d, u_q, i_d, i_q, u_f and i_f, the estimation models for the *d*- and *q*-axis are established separately. First, the armature and field winding flux linkages are determined by numerical integration of the following equations [8,21-25]

$$\frac{d\psi_d}{dt} = u_d + \omega\psi_q + R_s i_d \quad (8)$$

$$\frac{d\psi_q}{dt} = u_q - \omega\psi_d + R_s i_q \tag{9}$$

$$\frac{d\psi_f}{dt} = u_f - R_f i_f \tag{10}$$

where R_s is the stator resistance, ψ_d and ψ_q are the flux linkages in the *d*- and *q*-axis, respectively.

When ψ_d, ψ_q and ψ_f are known, the estimation models for the *d*- and *q*-axis can be established [8]. The *d*-axis estimation model is given by

$$0 = \hat{R}_D i_D + \frac{d\psi_D}{dt} \tag{11}$$

$$i_D = \frac{1}{L''_D}\left(\psi_D - \frac{k_d L_{\sigma s}}{L_{\sigma f} + k_d L_{\sigma s}}\psi_f - \frac{k_d L_{\sigma f}}{L_{\sigma f} + k_d L_{\sigma s}}\psi_d\right) \tag{12}$$

$$\hat{i}_f = \frac{1}{L''_f}\left(\psi_f - \frac{k_d L_{\sigma s}}{\hat{L}_{\sigma D} + k_d L_{\sigma s}}\psi_D - \frac{k_d \hat{L}_{\sigma D}}{\hat{L}_{\sigma D} + k_d L_{\sigma s}}\psi_d\right) \tag{13}$$

$$\hat{i}_d = \frac{1}{L''_d}\left(\frac{k_f \hat{L}_{\sigma D}}{\hat{L}_{\sigma D} + k_f L_{\sigma f}}\psi_f + \frac{k_f L_{\sigma f}}{\hat{L}_{\sigma D} + k_f L_{\sigma f}}\psi_D - \psi_d\right) \tag{14}$$

where ψ_D and i_D are the *d*-axis damper winding flux linkage and current, respectively, and

$$k_f = \frac{L_{md}}{L_{\sigma f} + L_{md}} \tag{15}$$

$$L''_d = L_{\sigma s} + \frac{1}{\frac{1}{L_{md}} + \frac{1}{L_{\sigma f}} + \frac{1}{\hat{L}_{\sigma D}}} \tag{16}$$

$$L''_f = L_{\sigma f} + \frac{1}{\frac{1}{L_{md}} + \frac{1}{L_{\sigma s}} + \frac{1}{\hat{L}_{\sigma D}}} \tag{17}$$

$$L''_D = \hat{L}_{\sigma D} + \frac{1}{\frac{1}{L_{md}} + \frac{1}{L_{\sigma s}} + \frac{1}{L_{\sigma f}}} \tag{18}$$

Similarly, *q*-axis estimation model can be written as

$$0 = \hat{R}_Q i_Q + \frac{d\psi_Q}{dt} \tag{19}$$

$$i_Q = \frac{1}{\hat{L}_{\sigma Q} + k_q L_{\sigma s}}\left(\psi_Q - k_q \psi_q\right) \tag{20}$$

$$\hat{i}_q = \frac{1}{L_{\sigma s} + k_Q \hat{L}_{\sigma Q}}\left(\psi_q - k_Q \psi_Q\right) \tag{21}$$

where ψ_Q and i_Q are the *q*-axis damper winding flux linkage and current, respectively, and

$$k_q = \frac{L_{mq}}{L_{\sigma s} + L_{mq}} \tag{22}$$

$$k_Q = \frac{L_{mq}}{\hat{L}_{\sigma Q} + L_{mq}} \tag{23}$$

where L_{mq} is the mutual inductance in the *q*-axis.

The input variables of the estimation model (11)-(18) are the flux linkages ψ_d and ψ_f. The currents $\hat{i}_d$ and $\hat{i}_f$ are the output variables and the flux linkage ψ_D is the state variable. In the estimation model (19)-(23) ψ_q is the input variable, $\hat{i}_q$ is the output variable and ψ_Q is the state variable. If the linearity is satisfied, all parameters in above established models are constant and the separate estimation procedures can be performed to identify damper winding parameters (R_D, $L_{\sigma D}$, R_Q, $L_{\sigma Q}$).

The estimation models (5)-(7), (11)-(18) and (19)-(23) were tested by using synthetic data (without noise corruption) obtained by the machine standard model simulations. For the purpose of parameters estimation Levenberg-Marquardt curve-fitting algorithm has been used [30]. By this testing, the perfect estimates are obtained for all the parameters of the standard machine model.

3 MATHEMATICAL MODEL OF ONE-SATURATED-GENERATOR INFINITE-BUS SYSTEM

3.1 Modelling of saturation

In order to investigate the influence of saturation on the rotor body parameters estimation, it is of great importance to have a reliable mathematical model of the saturated synchronous machine. The nonlinear variation of the saturated mutual inductances in the *d*- and *q*-axis, identified by on-line estimation presented in subsection 2.1, can be used for saturation model development. In the papers dealing with this subject, two different approaches can be found. A neural network approach is presented in references [15-17] and an analytical approach in references [21,26,27]. The later one is used in this study to establish mathematical model of the saturated synchronous machine.

Hence, in accordance with subsection 2.1, firstly, saturated synchronous inductances L_d and L_q are estimated from a total of 88 steady-state operating points measured on the 34 MVA generator in HPP Peruća. Based on these estimates the machine saturation characteristics can be obtained in the following form [21,31]

$$\psi_{md} = L_{md}(i_{md}, i_{mq}) \cdot i_{md} \tag{24}$$

$$\psi_{mq} = L_{mq}(i_{mq}, i_{md}) \cdot i_{mq} \tag{25}$$

where ψ_{md} and ψ_{mq} are the main flux linkages in the *d*- and *q*-axis, respectively. The magnetizing current in the *d*-axis (i_{md}) and *q*-axis (i_{mq}) may be expressed in per-unit system as follows

$$i_{md} = i_f + i_D - i_d \tag{26}$$

$$i_{mq} = i_Q - i_q \tag{27}$$

where i_f is the field current in per-unit on the reciprocal system of Rankin [2]. Note that under steady-state condition i_D and i_Q are equal zero. The mutual inductances in (24) and (25) are obtained from estimated values of L_d and L_q as

$$L_{md} = L_d - L_{\sigma s} \tag{28}$$

$$L_{mq} = L_q - L_{\sigma s} \tag{29}$$

Based on estimates for L_d and L_q, and measured values of i_{md} and i_{mq} the machine saturation characteristics are modelled by the polynomial functions in two variables as follows [26,27]

$$L_d = \sum_{j=1}^{m}(j+1)i_{md}^{j-1} \sum_{k=1}^{m} c_{jk} i_{mq}^{k+1} + C_1 \tag{30}$$

$$L_q = \sum_{j=1}^{m} i_{md}^{j+1} \sum_{k=1}^{m} c_{jk}(k+1) i_{mq}^{k-1} + C_2 \tag{31}$$

where m is positive integer defining the order ($2m$) of the polynomial functions, c_{jk}, C_1, and C_2 are the polynomial coefficients. These coefficients are determined by using the linear least-squares fitting technique [26]. Above polynomials satisfy the reciprocity property [31], which is immanent to the conservative magnetic field, and consequently they are valid for the saturation modelling in dynamic conditions.

For the generator under the test, the fitting surfaces for saturated synchronous inductance in the *d*- and *q*-axis are obtained and shown in Fig. 2. In the region of measurements, these surfaces are well matched with the measurements at all the considered 88 points. This region is bounded with dashed line in Fig. 2. The overall average discrepancy is less than 1%. From Fig. 2 it can be seen that the cross-magnetizing phenomenon has a considerable influence on both the *d*- and *q*-axis mutual inductances. As can be seen, both surfaces significantly deviate

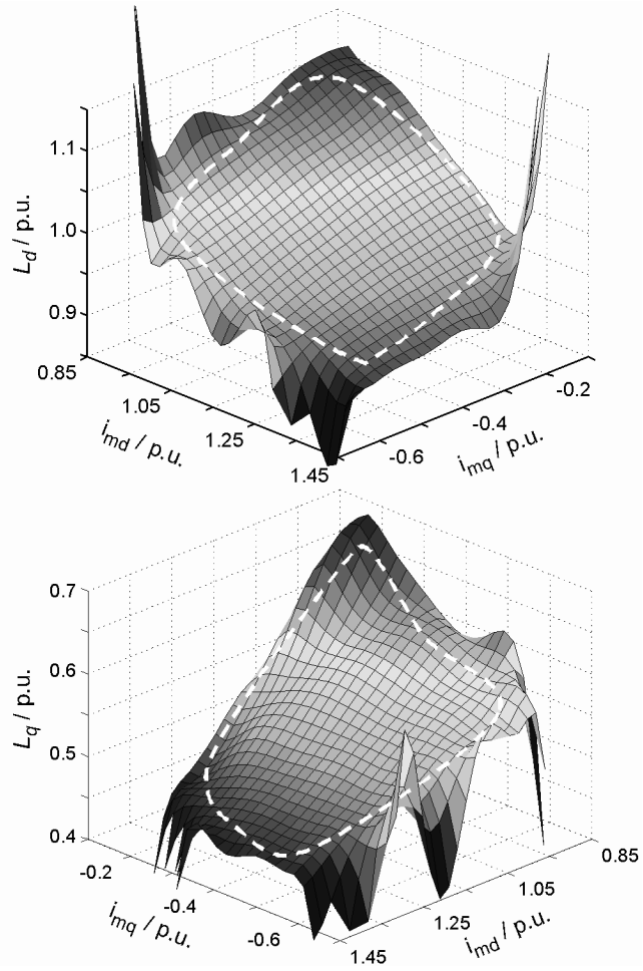

Fig. 2. Variation of saturated synchronous inductances as function of i_{md} and i_{mq}

outside dashed line due to the lack of the measured operating points and the high order of the polynomial functions ($2m = 16$). Polynomials (30) and (31) can be significantly simplified without reducing overall accuracy of saturation characteristics if reciprocity condition is neglected. By neglecting this condition following polynomials are obtained [26,27]

$$L_d = \sum_{j=0}^{m} i_{md}^{j} \sum_{k=0}^{n} a_{jk} i_{mq}^{k} \tag{32}$$

$$L_q = \sum_{j=0}^{m} i_{mq}^{j} \sum_{k=0}^{n} b_{jk} i_{md}^{k} \tag{33}$$

where m and n are positive integers defining the order ($m+n$) of the polynomial functions, a_{jk} and b_{jk} ($j = 0, 1, 2 \ldots m$, $k = 0, 1, 2 \ldots n$) are the polynomial coefficients given in Appendix A. By comparison to (30) and (31), coefficients of polynomial (32) and (33) are determined separately for the *d*- and *q*-axis using the linear

least-squares fitting technique. For the machine under the test the overall average discrepancy of the fitting surfaces, defined by (32) and (33), from the measurements is less than 0.5%.

For the sake of simplicity, from this point forward we will refer to polynomials (30) and (31) as "dynamic saturation model", and to polynomials (32) and (33) as "steady-state saturation model".

3.2 Model of saturated salient-pole synchronous machine

Now, previously presented saturation model will be implemented in the standard mathematical model of the salient-pole synchronous machine. Assuming positive stator current is out of terminals, as shown in Fig. 4, the voltage equations, in per-unit system and the rotor reference frame, may be expressed in matrix form as [21-25]

$$\frac{d\psi}{dt} = u - Ri + e \tag{34}$$

where

$$\psi = [\psi_d,\ \psi_f,\ \psi_D,\ \psi_q,\ \psi_Q]^{\mathrm{T}}$$

$$i = [-i_d,\ i_f,\ i_D,\ -i_q,\ i_Q]^{\mathrm{T}}$$

$$u = [u_d,\ u_f,\ 0,\ u_q,\ 0]^{\mathrm{T}}$$

$$e = [\omega\psi_d,\ 0,\ 0,\ -\omega\psi_q,\ 0]^{\mathrm{T}}$$

$$R = \mathrm{diag}(R_s,\ R_f,\ R_D, R_s,\ R_Q)$$

Subsequently, the equation of motion may be written as

$$\frac{d\omega}{dt} = \frac{1}{2H}\left(M_T - M_e\right) \tag{35}$$

where H is the inertia constant, M_T is the externally applied mechanical torque, and the electromagnetic torque is defined by

$$M_e = \psi_d i_q - \psi_q i_d \tag{36}$$

The relationship between the flux linkages and winding currents in the *d*-and *q*-axis may be arranged into the matrix form as follows

$$\begin{bmatrix} -i_d \\ i_f \\ i_D \end{bmatrix} = \begin{bmatrix} L_{\sigma s}+L_{md} & L_{md} & L_{md} \\ L_{md} & L_{\sigma f}+L_{md} & L_{md} \\ L_{md} & L_{md} & L_{\sigma D}+L_{md} \end{bmatrix}^{-1} \cdot \begin{bmatrix} \psi_d \\ \psi_f \\ \psi_D \end{bmatrix} \tag{37}$$

$$\begin{bmatrix} -i_q \\ i_Q \end{bmatrix} = \begin{bmatrix} L_{\sigma s}+L_{mq} & L_{mq} \\ L_{mq} & L_{\sigma Q}+L_{mq} \end{bmatrix}^{-1} \cdot \begin{bmatrix} \psi_q \\ \psi_Q \end{bmatrix} \tag{38}$$

In standard mathematical model, the mutual inductances L_{md} and L_{mq} are assumed to be constant. In order to implement saturation effects into the standard mathematical model, L_{md} and L_{mq} have to be expressed as functions of the magnetizing currents i_{md} and i_{mq} according to the "dynamic" or "steady-state" saturation model, taking into account relations (28) and (29).

Based on (26) and (27) it is clear, from simulation standpoint, that an iterative procedure is needed to calculate currents in (37) and (38). Obviously, it is not possible to find solution for the *d*-axis winding currents separately from the *q*-axis winding currents. A block diagram depicting the proposed iterative method for calculation of the currents in both axes is shown in Fig. 3. Hence, the procedure begins by assuming the initial values for currents equal to those in the previous integration step while the flux linkages are presumed to be known. Thereafter, the loop needs to carry on until the convergence of all the currents is attained. It should be pointed out that the iterative procedure illustrated in Fig. 3 is a bottleneck in the computer simulation since it needs to be carried out during each integration step.

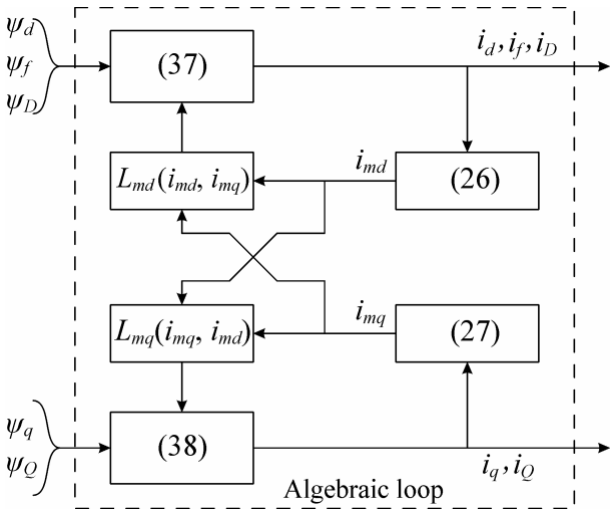

Fig. 3. Simulation of saturation in both axes of a salient-pole synchronous machine

3.3 Generator connection to infinite bus

In this section a model of transmission line connecting the synchronous generator to an infinite bus will be developed. This is necessary when generator with automatic

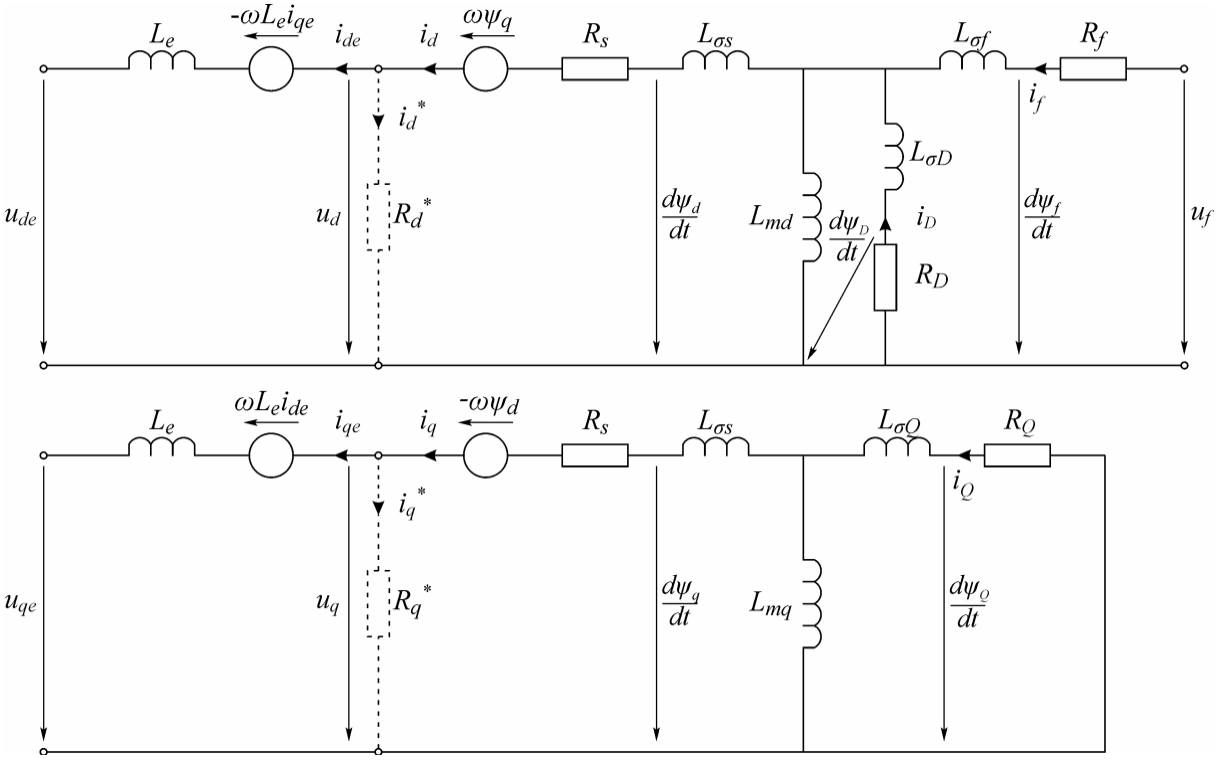

Fig. 4. Equivalent-circuit models in d- and q-axis of synchronous generator connected to infinite bus

voltage regulator is considered. In addition, this model provides terminal voltage calculation for the purpose of the identification algorithm testing. In order to establish this model the network under consideration should be replaced with Thevenin equivalent circuit. Besides, it is necessary to introduce the fictitious resistors R_d^* and R_q^* across the generator terminals as shown in Fig. 4. In that way it is possible to calculate the terminal voltages which are the input variables of the generator mathematical model (34)-(38).

By introducing the fictitious resistors two additional state variables (i_{de}, i_{qe}) are appeared, and two new voltage equations should be written as follows

$$\frac{di_{de}}{dt} = \frac{1}{L_e}\left(u_d - u_{de} + \omega\, L_e i_{qe}\right) \tag{39}$$

$$\frac{di_{qe}}{dt} = \frac{1}{L_e}\left(u_q - u_{qe} - \omega\, L_e i_{qe}\right) \tag{40}$$

where L_e is the equivalent transmission line inductance. For simplicity, the lossless transmission line is assumed.

The *d*- and *q*-components of Thevenin voltage (u_{de}, u_{qe}) are the input variables of the one-generator infinite-bus system model and can be expressed as

$$u_{de} = U_e \sin\delta_e \tag{41}$$

$$u_{qe} = U_e \cos\delta_e \tag{42}$$

where δ_e is the rotor angle defined as the electrical angular displacement of the rotor relative to the space vector of Thevenin voltage. Consequently,

$$\frac{d\delta_e}{dt} = \omega - \omega_e \tag{43}$$

where ω_e is the electrical angular velocity of Thevenin voltage.

Now, the *d*- and *q*-components of terminal voltage and the generator power angle (δ) are the output variables and can be calculated as follows

$$u_d = R_d^*\left(i_d - i_{de}\right) \tag{44}$$

$$u_q = R_q^*\left(i_q - i_{qe}\right) \tag{45}$$

$$\delta = \tan^{-1}\frac{u_d}{u_q} \tag{46}$$

It has been found out that a satisfactory accuracy is assured if values of the fictitious resistors are chosen as follows

$$R_d^* = 1000\; u_{do}/i_{do} \tag{47}$$

$$R_q^* = 1000\ u_{qo}/i_{qo} \tag{48}$$

where u_{do}, u_{qo}, i_{do}, i_{qo} are the voltages and currents at the initial operating point. By increasing the values of R_d^* and R_q^* a slight improvement of the simulation accuracy can be obtained, but this can also result in numerical instability.

3.4 Excitation system

In order to simulate the excitation disturbance that can be performed on the generator in real plant it is necessary to model the generator excitation system. For the considered 34 MVA generator in HPP Peruća the field winding is supplied from a three-phase fully controlled thyristor bridge which is connected to the generator terminals by the excitation transformer.

The excitation system model must be suitable for representing the actual excitation equipment performance for large disturbances as well as for small perturbations. In reference [32] the excitation system models suitable for use in large-scale system stability studies are presented. These model structures are intended to facilitate the use of field test data as a means of obtaining model parameters. In accordance with reference [32], the analogue static excitation system model of type ST1A and the corresponding digital version of type ST5B are taken into consideration. For simplicity, all the inputs except the terminal voltage reference are neglected. A much-simplified version of the considered excitation system and generator is shown in Fig. 5 in form of the transfer function block diagram. As can be seen, the excitation system is represented with the transfer function of proportional-integral (PI) controller, where the proportional gain K_P includes the controller and static exciter gain, T_I is the integral time of controller, $U_{f\min}$ and $U_{f\max}$ are the field voltage limits. The T_U is the time constant of the terminal voltage transducer.

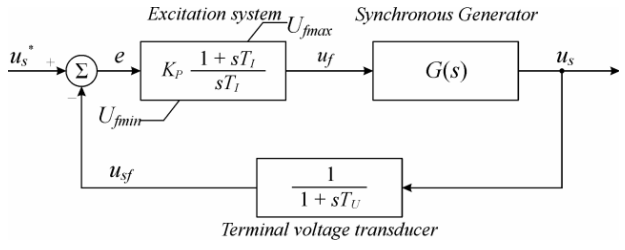

Fig. 5. Simplified block diagram of excitation system and generator

Note that corresponding of the symbols of the parameters used in this paper and their values are given in Appendix B.

4 INFLUENCE OF SATURATION ON ROTOR BODY PARAMETERS ESTIMATION

The identification procedure presented in section 2 can be also applied under saturated conditions. In comparison with the linear estimation models, the only difference is that the parameters of the estimation models are not constant under saturated conditions.

4.1 Field winding parameters

In the field winding estimation model defined in (5)-(7), the k_d is only coefficient that depends on the mutual inductances, i.e. on an operating point. Accordingly, based on (5)-(7), the field winding estimation model of the saturated machine can be established as follows

$$\Delta u_f = R_f \Delta\hat{i}_f + \frac{d\Delta\psi_f}{dt} \tag{49}$$

$$\begin{aligned}\Delta\hat{i}_f &= \tfrac{1}{\hat{L}_{\sigma f}+k_{do}L_{\sigma s}}\cdot \\ &\cdot\left[\Delta\psi_f - \tfrac{k_{do}\Delta u_q}{\omega_s} - \Delta k_d\left(L_{\sigma s}i_{fo} + \tfrac{k_{do}u_{qo}}{\omega_s}\right)\right]\end{aligned} \tag{50}$$

$$\Delta k_d = k_d(i_{fo}+\Delta\hat{i}_f, i_{do}+\Delta i_d, i_{qo}+\Delta i_q) - k_{do} \tag{51}$$

where index *o* denotes values at the initial operating point.

Since Δk_d is function of $\Delta\hat{i}_f$, an iteration procedure should be applied to solve equation (50). This can be avoided if the measured field current (Δi_f), instead of the estimated one ($\Delta\hat{i}_f$), is used in (51). In that way k_d becomes a known function of the measured armature and field winding currents. This makes that the estimation process becomes more stable and robust.

The testing of the estimation algorithm, for both the field and damper winding parameters, is performed by using synthetic data in three stages. First, the algorithm is tested with synthetic data generated by the one-machine infinite-bus system model simulation where the same ("dynamic") saturation model is used for the generator modelling and establishing of the estimation algorithm.

To provide synthetic data for testing of the field winding estimation algorithm, the field side of the machine should be disturbed in such a way that the contribution of damper winding currents can be neglected. This can be performed by a linear increase of the field voltage or current. Such simulated disturbance responses, which have been used for synthetic data generation, are shown in Fig. 6. By performing the first stage of testing, it has been shown that the estimation is possible to be performed and the deviations of the estimates from their true values are negligible.

The second stage of algorithm testing is to implement the estimation process with the same synthetic data as in the first stage and with the estimation algorithm established by using the "steady-state saturation model" which slightly

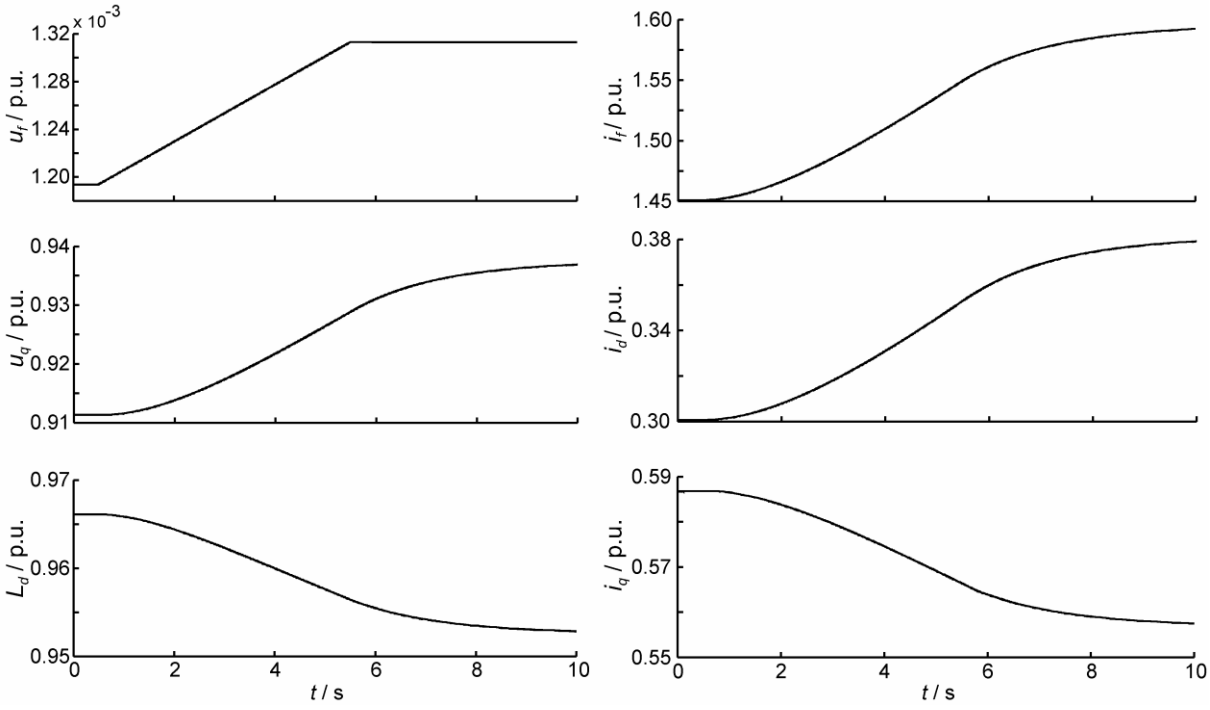

Fig. 6. Simulated disturbance responses used for synthetic data generation in order to estimate $L_{\sigma f}$ performed in operating point $U_s = 0.962$ p.u., $P = 0.627$ p.u., $Q = 0.093$ p.u.

differs from the "dynamic" one. In that way, the influence of slight deviations between two considered saturation models on the estimation process has been tested.

Finally, synthetic data are noise corrupted and then the effect of noise on the estimation process is evaluated. For that purpose the following noise corruption equation is used [18]

$$s_n(k) = s(k) + \left|\frac{s(k)}{SNR}\right| w(k) \tag{52}$$

where s_n and s represent noise corrupted and noise free measurements, respectively, SNR is the signal to noise ratio, and *w*(k) is the white noise signal with normal distribution.

Table 1 depicts the estimated parameters, obtained by using both the linear (5)-(7) and nonlinear estimation model (49)-(51). As can be seen from Table 1, the estimated value of the field winding leakage inductance is reasonably reliable up to SNR = 200:1 when estimation model (49)-(51) is applied. If the linear estimation model is used, the error obtained in case of no noise corruption is about 10%. According to that, it can be concluded that the influence of the saturation should be taken into account when the field winding leakage inductance is estimated. In accordance with Fig. 10, it has been found out that the noise level in the case of the machine under the test is too high to accurately estimate the field leakage inductance (SNR<100:1). Future work will involve investigation and application of new algorithms and techniques in order to decrease influence of measurement noise on the estimation procedure for obtaining $L_{\sigma f}$.

Table 1. Estimates of field winding parameter $L_{\sigma f}$

Case		Estimates (p.u.)	Error (%)
Noise Free	Linear	0.166	−9.3
	Nonlin.	0.182	−0.5
$SNR =$ 1000:1	Linear	$0.166 \leftrightarrow 0.167$	$-9.3 \leftrightarrow -8.7$
	Nonlin.	$0.182 \leftrightarrow 0.183$	$-0.5 \leftrightarrow +0.0$
$SNR =$ 500:1	Linear	$0.166 \leftrightarrow 0.168$	$-9.3 \leftrightarrow -8.2$
	Nonlin.	$0.182 \leftrightarrow 0.184$	$-0.5 \leftrightarrow +0.5$
$SNR =$ 200:1	Linear	$0.170 \leftrightarrow 0.173$	$-7.1 \leftrightarrow -5.5$
	Nonlin.	$0.185 \leftrightarrow 0.188$	$+1.1 \leftrightarrow +2.7$
$SNR =$ 100:1	Linear	$0.181 \leftrightarrow 0.191$	$-1.1 \leftrightarrow +4.3$
	Nonlin.	$0.193 \leftrightarrow 0.201$	$+5.4 \leftrightarrow +9.8$
$SNR =$ 50:1	Linear	$0.220 \leftrightarrow 0.234$	$+20 \leftrightarrow +28$
	Nonlin.	$0.227 \leftrightarrow 0.240$	$+24 \leftrightarrow +31$

4.2 Damper winding parameters

Under saturated conditions, the damper winding estimation model becomes more complex in comparison with the field winding one. Seven parameters of the estimation

model, described by (11)-(14) and (19)-(21), depend on variation of the saturated mutual inductances in the *d*- and *q*-axis. Since data are generated under subtransient conditions when all the machine windings are excited, it may be written

$$\begin{aligned} k_d &= k_d(i_d, i_f, \hat{i}_D, i_q, \hat{i}_Q) \\ k_f &= k_f(i_d, i_f, \hat{i}_D, i_q, \hat{i}_Q) \\ k_q &= k_q(i_d, i_f, \hat{i}_D, i_q, \hat{i}_Q) \\ k_Q &= k_Q(i_d, i_f, \hat{i}_D, i_q, \hat{i}_Q) \\ L''_d &= L''_d(i_d, i_f, \hat{i}_D, i_q, \hat{i}_Q) \\ L''_f &= L''_f(i_d, i_f, \hat{i}_D, i_q, \hat{i}_Q) \\ L''_D &= L''_D(i_d, i_f, \hat{i}_D, i_q, \hat{i}_Q) \end{aligned} \tag{53}$$

where i_d, i_f and i_q are the measured, and $\hat{i}_D$, $\hat{i}_Q$ are the estimated currents. Besides, due to the cross-magnetization caused by saturation, the separate estimation models for the *d*- and *q*-axis are not possible. Thus, the parameters R_D, $L_{\sigma D}$, R_Q, $L_{\sigma Q}$ should be estimated together. Accordingly, the cost function of estimation error can be stated as follows

$$\begin{aligned} \Delta Y(\hat{R}_D, \hat{L}_{\sigma D}, \hat{R}_Q, \hat{L}_{\sigma Q}) = \sum_{k=1}^{N} \left(\hat{i}_f(\hat{R}_D, \hat{L}_{\sigma D}) - i_f \right)_k^2 + \\ + \sum_{k=1}^{N} \left(\hat{i}_d(\hat{R}_D, \hat{L}_{\sigma D}) - i_d \right)_k^2 + \sum_{k=1}^{N} \left(\hat{i}_q(\hat{R}_Q, \hat{L}_{\sigma Q}) - i_q \right)_k^2 \end{aligned} \tag{54}$$

where N is the number of measured points taken into account.

Due to saturation, the coefficients of estimation model depend on the damper winding currents which are not measurable and should be estimated. Because of that an iteration procedure should be applied to solve the system of two nonlinear algebraic equations, (12) and (20), for currents i_D and i_Q, respectively. The block diagram of the estimation algorithm for damper winding is shown in Fig. 7.

To provide synthetic data for testing of the damper winding identification algorithm, the field side of the machine should be disturbed in such a way that considerable currents in the damper winding are excited. In this study, consecutive changes of the terminal voltage reference are provided for that purpose (Fig. 8). First, terminal voltage reference is decreased for 5% and after time t_1 it is increased to the initial value and again, after t_1, decreased for 5%.

In that way a large excitation disturbance is performed. The corresponding simulated responses of the variables which are used as measurements in the estimation models, (11)-(23) and (53), are shown in Fig. 9. These responses are obtained by using the mathematical model of the one-saturated-generator infinite-bus system described in section 3. It should be noted that a very slight difference exists between the responses obtained by both the "dynamic" and "steady-state" saturation models.

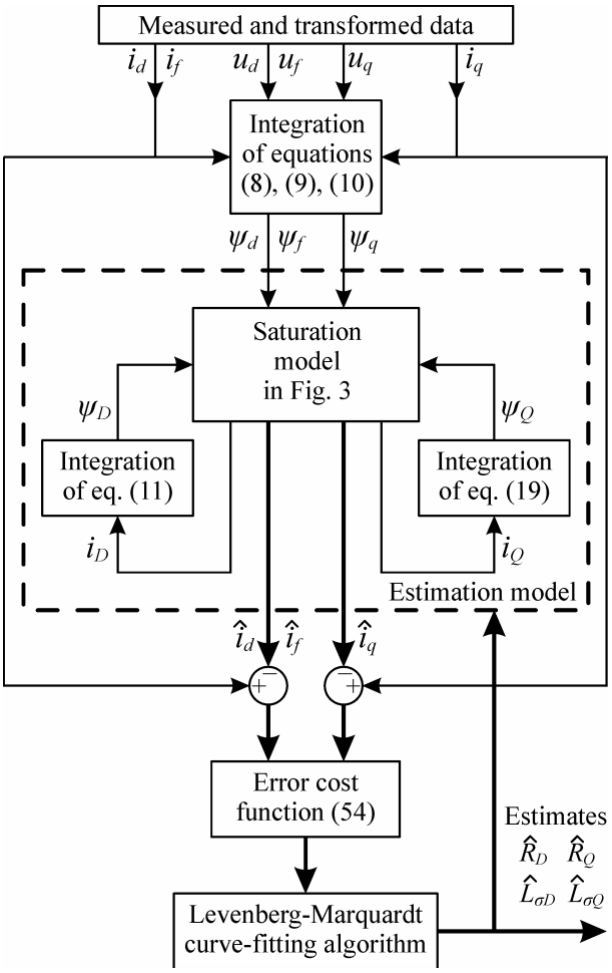

Fig. 7. Block diagram of estimation algorithm for damper winding

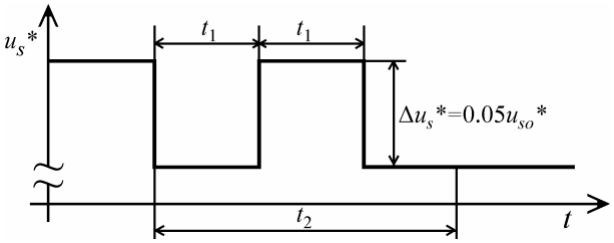

Fig. 8. Illustration of changes of terminal voltage reference used in simulations

By performing the first stage of testing of the damper winding identification algorithm, which is described in subsection 4.1, it has been shown that the estimation is possible to be performed and the deviations of the estimates from their true values are negligible. The linear estimation models (11)-(14) and (19)-(21) have also been tested and it has been shown that the estimation does not work

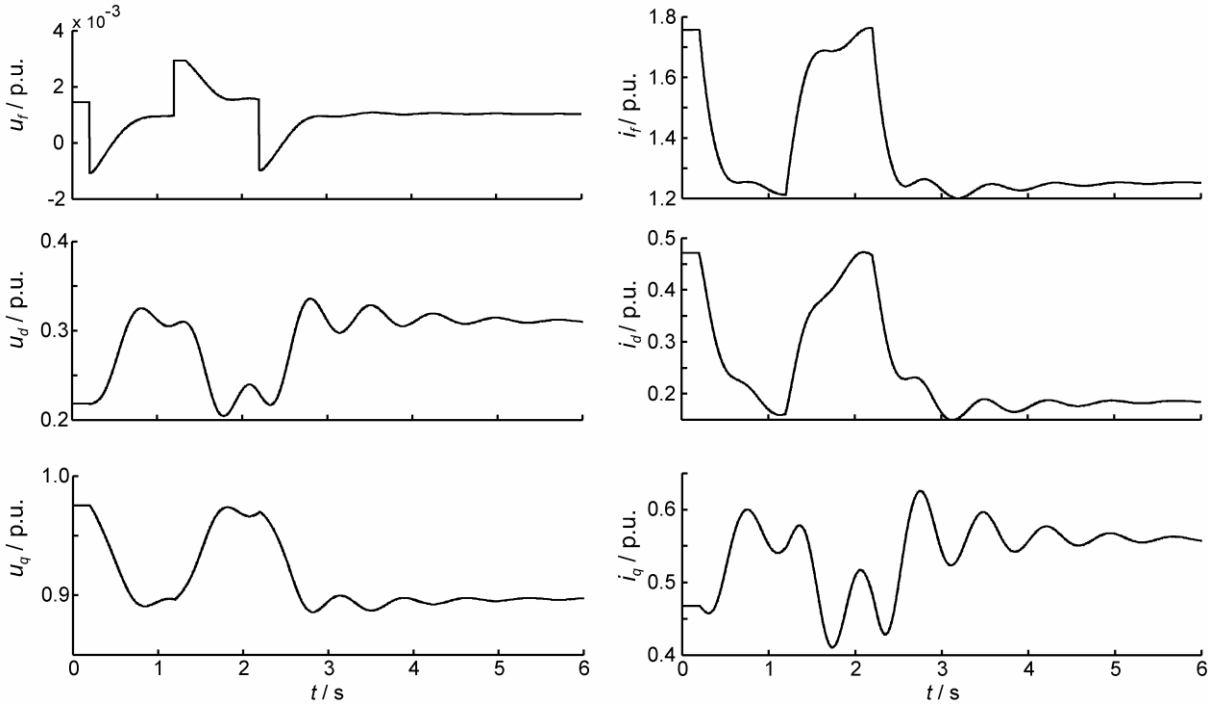

Fig. 9. Simulated disturbance responses during consecutive changes of terminal voltage reference depicted in Fig. 8 for t_1 = 1 s, performed in operating point $U_s = 0.999$ p.u., $P = 0.559$ p.u., $Q = 0.358$ p.u.

under saturated conditions. The second stage of the algorithm testing has been performed for three different disturbances, which are created by changing parameters t_1 and t_2 of the pattern shown in Fig. 8. The estimation errors of the damper winding parameters are shown in Table 2. Obviously, the damper winding estimates strongly depend on kind of the performed excitation disturbance, particularly the *d*- and *q*-axis leakage inductances. It should be pointed out that the errors of the estimates are caused by a slight deviation between two applied generator saturation models; the "dynamic saturation model" is used to generate synthetic data and the "steady-state saturation model" is used in the estimation algorithm.

Based on the presented results for the damper winding estimates it can be concluded that an accurate estimation is only possible if the identified machine saturation characteristic perfectly matches the actual one. This shows that measurements performed with standard equipment, with common accuracy of e.g. 1%, used to identify the machine saturation characteristics, would not be accurate enough for the estimation purpose. In addition, it should be emphasized that the results presented in Table 2 have been obtained by using data without noise corruption.

It is well known that the measurement noise reduces the robustness of estimation process and can cause that the estimation is not possible to be performed. For instance, such a case is measurement data obtained in HPP Peruća. The machine variables responses during the large excitation disturbance performed by the sudden change in the terminal voltage reference by 2% are shown in Fig. 10. By thoroughly analysis of the measured signals it has been found out that the noise level is too high to be used for the estimation purpose ($SNR < 100 : 1$). Thus, according to the investigations presented in this paper it can be concluded that validation of the methods for the damper winding parameters on-line estimation, which have been presented in papers dealing with this subject, are questionable.

Table 2. Estimation error of damper winding parameters

t_1 (s)	t_2 (s)	Estimation error (%)			
		ΔR_D	$\Delta L_{\sigma D}$	ΔR_Q	$\Delta L_{\sigma Q}$
1.00	3.00	4.4	−39	−6.9	−1.3
	2.00	−3.6	−43	−0.9	23
	1.00	27	−25	−17	−50
0.75	2.25	6.6	−32	−8.5	18
	1.50	−1.6	−44	−4.8	65
	0.75	26	−20	−16	−60
0.50	1.50	6.4	−41	−7.5	28
	1.00	0.1	−51	−7.2	27
	0.50	19	0.9	−9.4	−51

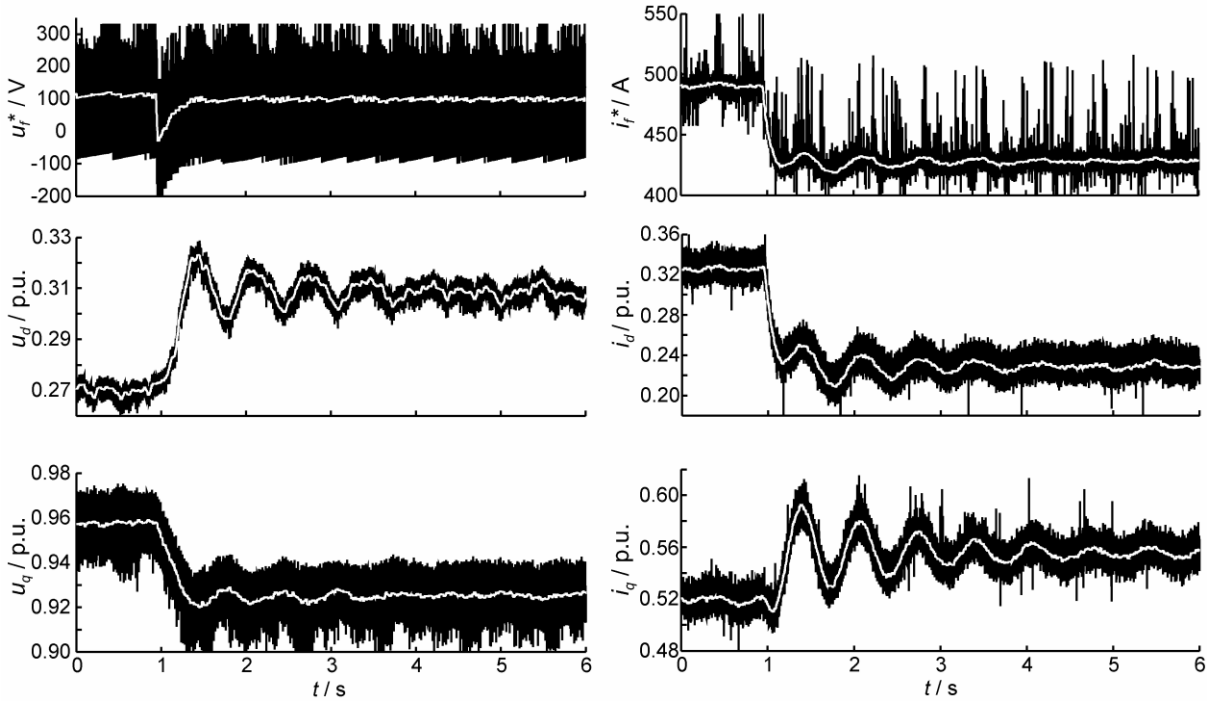

Fig. 10. Measured (black) and smoothed (white) machine variables responses during large excitation disturbance performed in operating point $U_s = 0.994$ p.u., $P = 0.585$ p.u., $Q = 0.167$ p.u.

5 CONCLUSIONS

Based on an analytical saturation model, nonlinear identification algorithms for the rotor body parameters of the synchronous hydro-generator are developed. These algorithms have been tested using synthetic data obtained by the one-generator infinite-bus system model simulation. It has been shown that the wrong estimates are obtained if the linear estimation model is used under saturated conditions, particularly for the damper winding parameters. In other words, under saturated conditions the nonlinear estimation model for field and damper winding have to be used. Also, an influence of the saturation model accuracy on the estimation process has been investigated. This study has shown that a small deviation of the identified generator saturated characteristic from the actual one, which is inside of the measurement accuracy boundaries, can cause a large error in the estimates of the damper winding. Particularly, this is true for the damper winding leakage inductances. The same deviation of the saturation characteristic does not affect the estimation results for the field winding leakage inductance. In this way, it has been proved that an accurate estimation of the damper winding parameters, based on the field side machine disturbance data, is not possible under saturated conditions.

APPENDIX A - FITTING SURFACES COEFFICIENTS FOR "STEADY-STATE SATURATION MODEL"

By applying a procedure described in references [26,27] on the measurement data performed on the generator under the test, the coefficients of saturation characteristics (32) and (33) are calculated and given in tables 3 and 4.

Table 3. Coefficients of polynomial (32)

a_{jk}		k		
		0	1	2
j	0	1.581E+0	-5.986E-1	-1.387E+0
	1	-5.394E-1	1.297E+0	2.365E+0
	2	5.049E-2	-6.299E-1	-1.032E+0

Table 4. Coefficients of polynomial (33)

b_{jk}		k			
		0	1	2	3
j	0	-4.544E-1	6.496E+0	-8.642E+0	3.173E+0
	1	-3.300E-1	1.446E+1	-2.519E+1	1.068E+1
	2	4.610E+0	1.363E+1	-3.688E+1	1.760E+1
	3	3.781E-1	1.818E+1	-3.421E+1	1.494E+1

Table 5. One-generator infinite-bus simulation parameters

Machine parameters		
R_s	Armature winding resistance	0.0043
$L_{\sigma s}$	Armature winding leakage inductance	0.1360
R_f	Field winding resistance	0.0008
$L_{\sigma f}$	Field winding leakage inductance	0.1833
R_D	Damper winding resistance in *d*-axis	0.0083
$L_{\sigma D}$	Damper winding leakage inductance in *d*-axis	0.1089
R_Q	Damper winding resistance in *q*-axis	0.0190
$L_{\sigma Q}$	Damper winding leakage inductance in *q*-axis	0.1280
L_{md}	Direct axis magnetizing mutual inductance (unsaturated)	1.0125
L_{mq}	Quadrature axis magnetizing mutual inductance (unsaturated)	0.5840
H	Inertia constant	1068.1
a	Turns ratio	12.075
Transmission line parameters		
L_e	Transmission line inductance	0.1360
Excitation system parameters		
K_P	Proportional gain of PI controller	0.0500
T_I	Integral time of PI controller	314.16
T_U	Time constant of voltage transducer	6.2832

APPENDIX B - NOMENCLATURE AND VALUES OF PARAMETERS USED IN SIMULATIONS

The machine under the test is 32-pole hydroturbine generator, and its nominal ratings are as follows: 34 MVA, 10.5 kV, 1870 A, power factor 0.9 and 187.5 rpm. The parameters of the hydro-generator along with its excitation system and transmission line parameters used in the simulations are listed in Table 5. All the parameters are referred to the stator and are expressed in per-unit [21-25].

ACKNOWLEDGEMENTS

The authors acknowledge the assistance of the staff of the HPP Peruća and the engineers of Končar-INEM Company for their contribution during setup of the large excitation disturbance experiment. The authors gratefully acknowledge the contributions of enthusiasts Goran Orešković and Boris Meško of VESKI Company for their work on setup of measurement equipment.

REFERENCES

[1] IEC Standard, Publication 34-4, Part 4: **Methods for determining synchronous machine quantities from tests**, Geneva, 1985.

[2] IEEE Standard 115-1995, **IEEE Guide: Test Procedures for Synchronous Machines**, New York, 1996.

[3] M. Dehghani, M. Karrari, W. Rosehart, O. P. Malik, **Synchronous machine model parameters estimation by a time-domain identification method**, International Journal of Electrical Power & Energy Systems, In Press, Available online 27 August 2009.

[4] M. A. Arjona, R. Escarela-Perez, G. Espinosa-Perez, J. Alvarez-Ramirez, **Validity testing of third-order nonlinear models for synchronous generators**, Electric Power Systems Research, vol. 79, no. 6, pp. 953-958, June 2009.

[5] M. Rahimpour, M. A. Talebi, H. A. Shayanfar, M. R. A. Hosseini, **On line synchronous generator parameters estimation based on applying small disturbance on excitation system using ANN**, Proc. of the 2009 IEEE PES Power Systems Conference and Exposition, Seattle, WA, USA, Mar. 15-18, 2009.

[6] S. Perez-Londono, A. Perez-Londono, Y. Romero-Mora, **On-line identification of the physical parameters in a synchronous generator**, Proc. of the 2008 IEEE PES Transmission and Distribution Conference and Exposition: Latin America, Bogota, Columbia, Aug. 13-15, 2008.

[7] M. Dehghani, S. K. Y. Nikravesh, **Nonlinear state space model identification of synchronous generators**, Electric Power Systems Research, vol. 78, no. 5, pp. 926-940, May 2008.

[8] M. Jadrić, M. Despalatović, B. Terzić, B. Rajković, **Methodology for Synchronous Hydrogenerator Parameter Identification Based on Monitoring System Measurement**, Automatika, vol. 48, No 1-2, pp. 9-19, 2007. In Croatian.

[9] M. A. Talebi, M. Rahimpour, A. Gholami, A. Vahedi, H. A. Shayanfar, **A Genetic Algorithm Approach for Identifying Synchronous Generator Parameters from Excitation Disturbance Test**, Proc. of the 2007 IEEE Power Engineering Society General Meeting, Tampa, FL, USA, June 24-28, 2007.

[10] S. A. Saied, S. M. Bathaee, M. Karrari, W. Rosehart, O. P. Malik, **Identification of Electric Parameters of Syn-**

chronous Generator Using Input_Output Data Set, Proc. of the 2006 IFAC Symposium on Power Plants and Power Systems Control, pp. 83-88, Kananaskis, Canada, 2006.

[11] M. Despalatović, M. Jadrić, B. Terzić, J. Macan, **On-line hydrogenerator power angle and synchronous reactances determination based on air gap measurements**, Proc. of the 2004 IEEE PES Power System Conference and Exposition, vol. 2, pp. 753-758, New York, NY, USA, Oct. 10-13, 2004.

[12] M. Karrari, O. P. Malik, **Identification of Physical Parameters of a Synchronous Generator From Online Measurements**, IEEE Trans. on Energy Conversion, vol. 19, no. 2, pp. 407-415, June 2004.

[13] M. Calvo, O. P. Malik, **Synchronous Machine Steady-State Parameter Estimation Using Neural Networks**, IEEE Trans. on Energy Conversion, vol. 19, no. 2, pp. 237-244, June 2004.

[14] E. Kyriakides, G. T. Heydt, **Estimation of synchronous generator parameters using an observer for damper currents and a graphical user interface**, Electric Power Systems Research, vol. 69, no. 1, pp.7-16, Apr. 2004.

[15] H. B. Karayaka, A. Keyhani, G. T. Heydt, B. L. Agrawal, D. A. Selin, **Synchronous Generator Model Identification and Parameter Estimation From Operating Data**, IEEE Trans. on Energy Conversion, vol. 18, no. 1, pp. 121-126, Mar. 2003.

[16] H. B. Karayaka, A. Keyhani, G. T. Heydt, B. L. Agrawal, D. A. Selin, **Neural Network Based Modeling of a Large Steam Turbine-Generator Rotor Body Parameters From On-Line Disturbance Data**, IEEE Trans. on Energy Conversion, vol. 16, no. 4, pp. 305-311, Dec. 2001.

[17] H. B. Karayaka, A. Keyhani, B. L. Agrawal, D. A. Selin, G. T. Heydt, **Identification of Armature, Field, and Saturated Parameters of a Large Steam Turbine-Generator from Operating Data**, IEEE Trans. on Energy Conversion, vol. 15, no. 2, pp. 181-187, June 2000.

[18] H. B. Karayaka, A. Keyhani, B. Agrawal, D. Selin and G. T. Heydt, **Methodology Development for Estimation of Armature Circuit and Field Winding Parameters of Large Utility Generators**, IEEE Trans. on Energy Conversion, vol. 14, No 4, pp. 901 - 908, December 1999.

[19] H. Tsai, A. Keyhani, J. Demecko and R. G. Farmer, **On-Line Synchronous Machine Parameter Estimation from Small Disturbance Operating Data**, IEEE Trans. on Energy Conversion, vol. 10, No 1, pp. 25 - 36, March 1995.

[20] Z. M. Zhao, F. S. Zheng, J. D. Gao and L. Y. Xu, **A Dynamic On-line Parameter Identification and Full-Scale System Experimental Verification For Large Synchronous Machines**, IEEE Trans. on Energy Conversion, vol. 10, No 3, pp. 392 - 398, September 1995.

[21] I. Boldea, **Synchronous Generators**, CRC/Taylor & Francis, Boca Raton, 2006.

[22] M. Jadrić, B. Frančić, **Dynamics of Electrical Machines**, Graphis, Zagreb, 2004. In Croatian.

[23] P. C. Krause, O. Wasynczuk, S. D. Sudhoff, **Analysis of Electric Machinery and Drive Systems** (2nd Edition), Wiley-IEEE Press, New York, 2002.

[24] C.-M. Ong, **Dynamic Simulation of Electric Machinery** (Using Matlab/Simulink), Prentice Hall, Upper Saddle River, 1998.

[25] P. Kundur, **Power System Stability and Control**, McGraw-Hill Inc., New York, 1994.

[26] M. Despalatović, **Identification of synchronous hydrogenerator parameters based on on-line measurements**, PhD thesis, Faculty of Electrical Engineering, Mechanical Engineering and Naval Architecture, Split, 2009. In Croatian.

[27] M. Jadrić, M. Despalatović, B. Terzić, **Development of synchronous generator saturation model from steady-state operating data**, Electric Power Systems Research, Submitted for review 16 Sep. 2008.

[28] M. Despalatović, M. Jadrić, B. Terzić, **Real-time power angle determination of salient-pole synchronous machine based on air gap measurements**, Electric Power Systems Research, vol. 78, no. 11, pp. 1873-1880, 2008.

[29] M. Jadrić, M. Despalatović, B. Terzić, J. Macan, **Determination of Synchronous Generator Armature Leakage Reactance Based on Air Gap Flux Density Signal**, Automatika, vol. 48, No 3-4, pp. 129-135, 2007.

[30] W. H. Press, S. A. Teukolsky, W. T. Vetterling, B. P. Flannery, **Numerical Recipes: The Art of Scientific Computing** (3rd Edition), Cambridge University Press, New York, 2007.

[31] J. A. Melkebeek, J. L. Willems, **Reciprocity Relations for the Mutual Inductances Between Orthogonal Axis Windings in Saturated Salient-Pole Machines**, IEEE Trans. on Industry Applications, vol. 26, no. 1, pp. 107-114, Jan./Feb. 1990.

[32] IEEE Standard 421.5-2005, **IEEE Recommended Practice for Excitation System Models for Power System Stability Studies**, New York, 2006.

Marin Despalatović was born in Split, Croatia, in 1976. He received the B.S. and Ph.D. degrees in electrical engineering from the Faculty of Electrical Engineering, Mechanical Engineering and Naval Architecture, University of Split, Split, Croatia, in 2000 and 2009, respectively. Since 2001 he has been in the Department of Electric Power Engineering at the University of Split as a Research Assistant. His research interests include electrical machines and drives, in particular, parameter estimation of electrical machines.

Martin Jadrić received the B.S. degree in electrical engineering from the University of Split, Split, Croatia, and the M.S. and Ph.D. degrees from the University of Zagreb, Zagreb, Croatia, in 1964, 1970, and 1976, respectively. After completing his graduate studies, he joined Končar Company, Zagreb, Croatia. Since 1996, he has been with the Faculty of Electrical Engineering, Mechanical Engineer ing and Naval Architecture, University of Split, first as an Assistant (through 1978), then as an Associate Professor (1978-1984), and currently as a Full Professor. During his career with the university, he has been responsible for the electric machines and drives curriculum, was the Head of the Department of Electric Power Engineering and, from 1980 to 1983, he was the Dean of the Faculty of Electrical Engineering, Mechanical Engineering and Naval Architecture. He has been involved in numerous government- and industry-sponsored projects in the areas of electrical machines and drives, and has authored more than 70 published technical papers and one book, Dynamics of Electrical Machines (in Croatian).

Božo Terzić was born in Grab, Croatia, in 1962. He received the B.S. and Ph.D. degrees in electrical engineering from the Faculty of Electrical Engineering, Mechanical Engineering and Naval Architecture, University of Split, Split, Croatia, in 1986 and 1998, respectively, and the M.S. degree from the Faculty of Electrical Engineering, University of Zagreb, Zagreb, Croatia, in 1993. In 1986, he became an Assistant in the Department of Electric Power Engineering, Faculty of Electrical Engineering, Mechanical Engineering and Naval Architecture, University of Split, where, since 2009, he has been a Full Professor. Currently, he is the Head of the Department of Electric Power Engineering. His research interests include ac electrical machines and drives.

AUTHORS' ADDRESSES

Marin Despalatović, Ph.D.
Prof. Martin Jadrić, Ph.D.
Prof. Božo Terzić, Ph.D.
Department of Electric Power Engineering,
Faculty of Electrical Engineering, Mechanical Engineering and Naval Architecture, University of Split,
Ruđera Boškovića bb, HR-21000 Split, Croatia
emails: marin.despalatovic@fesb.hr,
martin.jadric@fesb.hr, bozo.terzic@fesb.hr

Received: 2009-11-02
Accepted: 2009-11-27